THE JOURNAL OF BIOLOGICAL CHEMISTRY
Vol. 280, No. 20, Issue of May 20, pp. 19858–19866, 2005
Printed in U.S.A.

Recycling of the Membrane-anchored Chemokine, CX_3CL1*

Received for publication, November 19, 2004, and in revised form, February 15, 2005
Published, JBC Papers in Press, March 16, 2005, DOI 10.1074/jbc.M413073200

Guang-Ying Liu‡, Vathany Kulasingam‡, R. Todd Alexander‡, Nicolas Touret‡, Alan M. Fong§, Dhavalkumar D. Patel§, and Lisa A. Robinson‡¶

From the ‡The Hospital for Sick Children Research Institute and the University of Toronto, Toronto M5G 1X8, Canada and §Thurston Arthritis Research Center, The University of North Carolina, Chapel Hill, North Carolina 27599-7280

CX_3CL1 (fractalkine) plays an important role in inflammation by acting as both chemoattractant and as an adhesion molecule. As for other chemokines, expression of CX_3CL1 is known to be regulated at the level of transcription and translation. The unique transmembrane structure of CX_3CL1 raises the possibility of additional functional regulation by altering its abundance at the cell surface. This could be accomplished in principle by changes in traffic between subcellular compartments. To analyze this possibility we examined the subcellular distribution of CX_3CL1 in human ECV-304 cells stably expressing untagged or green fluorescent protein-tagged forms of the chemokine. CX_3CL1 was present in two distinct compartments, diffusely on the plasma membrane and in a punctate juxtanuclear compartment. The latter shared some features with, yet was distinct from the conventional endocytic pathway and may represent a specialized recycling subcompartment. Accordingly, surface CX_3CL1 was found to be in dynamic equilibrium with the juxtanuclear vesicular compartment. Intracellular CX_3CL1 co-localized with the SNARE (soluble *N*-ethylmaleimide factor attachment protein receptor) proteins syntaxin-13 and VAMP-3. Cleavage of VAMP-3 by tetanus toxin or impairment of syntaxin-13 function by expression of a dominant-negative allele inhibited the ability of internalized CX_3CL1 to traffic back to the plasma membrane. These data demonstrate the existence of a dynamic, SNARE-mediated recycling of CX_3CL1 from the cell surface to and from an endomembrane storage compartment. The intracellular storage depot may serve as a source of the chemokine that could be rapidly mobilized by stimuli.

Inflammation is marked by the migration of circulating leukocytes into sites of injury. The inflammatory process involves a series of coordinated interactions between leukocytes and endothelial or epithelial cells. Central to this sequence of events are chemokines, a family of low molecular weight proteins that function as attractants of leukocytes bearing the complementary receptors. When engagement of chemokine receptors occurs, leukocytes become activated and are induced to adhere firmly to the inflamed endothelium. These initial steps culminate in diapedesis of the leukocyte across the endothelium and migration into the injured tissue (1). The local complement of chemokines elaborated by each organ is specific and varies with the type of inflammation present (1). In addition, specific subsets of leukocytes bear distinct chemokine receptors. In this manner chemokines and their cognate receptors confer organ specificity to leukocyte migration and help to fine-tune the nature of the observed inflammatory response.

One such chemokine, CX_3CL1 (fractalkine) and its receptor, CX_3CR1, have been shown to be of central importance in diverse inflammatory and infectious disease processes. Interrupting this pathway *in vivo* has a highly protective effect in animal models of renal inflammation (2), rejection of transplanted organs (3, 4), and atherosclerosis (5, 6). Unlike most other chemokines, CX_3CL1 exists in two forms; as a soluble chemotactic polypeptide and as a transmembrane chemokine/mucin hybrid protein. In its soluble form, CX_3CL1 acts as a chemoattractant for leukocytes bearing its unique receptor, CX_3CR1 (7, 8). In the membrane-bound form, the mucin stalk allows the chemokine domain of CX_3CL1 to be efficiently presented to circulating leukocytes (9, 10). Membrane-associated CX_3CL1 has been shown to mediate multiple steps of the leukocyte adhesion cascade, including capture of circulating leukocytes, either alone or in concert with other adhesion molecules such as VCAM-1 (9, 11). After the initial recruitment step, CX_3CL1 interacts with CX_3CR1 to further promote activation and firm the arrest of monocytes, NK cells, and $CD8^+$ T lymphocytes (9). Thus, CX_3CL1 has dual roles as a chemoattractant and a cellular adhesion molecule.

Like other chemokines, CX_3CL1 biosynthesis is regulated at the transcriptional and translational levels (7, 9, 12–14). However, because of its unique transmembrane disposition, CX_3CL1 activity may be controlled by additional mechanisms. Indeed, it is conceivable that the surface exposure of the membrane-associated chemokine is regulated by traffic between subcellular compartments, as has been reported for a variety of membrane receptors and transporters (15–19). Remarkably, very little is known about the subcellular distribution and traffic of CX_3CL1.

The objective of the present study was, therefore, to characterize the subcellular distribution of CX_3CL1, its ability to translocate between cellular compartments, and the molecular determinants of this traffic. We found that CX_3CL1 actively cycles between the plasma membrane and an internal, vesicular pool and also characterized the soluble *N*-ethylmaleimide factor attachment protein receptors (SNARE)[1] proteins involved in this process. The implications of these findings for the regulation of CX_3CL1 function are discussed.

* The costs of publication of this article were defrayed in part by the payment of page charges. This article must therefore be hereby marked "*advertisement*" in accordance with 18 U.S.C. Section 1734 solely to indicate this fact.

¶ To whom correspondence should be addressed: Dept. of Paediatrics, The Hospital for Sick Children, 555 University Ave., Toronto, Ontario M5G 1X8, Canada. Tel.: 416-813-7654 (ext. 1745); Fax: 416-813-6271; E-mail: lisa.robinson@sickkids.ca.

[1] The abbreviations used are: SNARE, soluble *N*-ethylmaleimide factor attachment protein receptor; GFP, green fluorescent protein; EGFP, enhanced GFP; PAEC, primary porcine aortic endothelial cells; Ab, antibody; FRAP, fluorescence recovery after photobleaching; DN, dominant negative; TACE, tumor necrosis factor-converting enzyme.

EXPERIMENTAL PROCEDURES

Reagents and Antibodies—The following antibodies were used: goat polyclonal anti-CX_3CL1 (R&D Systems, Inc., Minneapolis, MN), anti-CD63 (Caltag Laboratories, Burlingame, CA), anti-GM130 (Transduction Laboratories, Lexington, KY), Cy3-, peroxidase-, and Alexa 488-conjugated anti-goat IgG (Jackson ImmunoResearch Laboratories, West Grove, PA; Molecular Probes, Inc., Eugene, OR), and Fab fragment of fluorescein isothiocyanate-conjugated anti-goat IgG (Jackson ImmunoResearch Laboratories, West Grove, PA).

Rhodamine-conjugated transferrin and nigericin were obtained from Molecular Probes, and colchicine, brefeldin, and *o*-phenylenediamine dihydrochloride were from Sigma. DNA expression constructs encoding GFP-tagged VAMP-3, VAMP-2, and syntaxin-13 as well as dominant negative-syntaxin-13 and mammalian tetanus toxin were generously provided by Dr. William S. Trimble (The Hospital for Sick Children Research Institute, Toronto, Ontario) and Dr. R. Scheller (Stanford University, Stanford, CA) (20–24). ECV-CX_3CL1 cells were transiently transfected with DNA encoding the above GFP-tagged proteins using FuGENE (Roche Diagnostics), and transfected cells were analyzed 24 h later. In separate experiments ECV-CX_3CL1 cells were transfected with EGFP alone or in combination with dominant negative-syntaxin-13 or tetanus toxin at a ratio of 1:10.

Cell Culture—ECV-304 cells were obtained from the American Type Culture Collection (Manassas, VA), and the generation of CX_3CL1-expressing ECV-304 cells (ECV-CX_3CL1) has been previously described (9). A plasmid encoding CX_3CL1-GFP hybrid molecules was generated by PCR and subsequent ligation of the DNA fragments into pEGFP-N2 (BD Biosciences Clontech). DNA encoding the extracellular and transmembrane portions of CX_3CL1 was synthesized using primers 5′-CGGGTCGACTCAGCCATGGCTCCGATA and 5′-CTGAGGATCCCC-ACGGGCACCAGGAC and digested with Sal1 and BamH1. These fragments were ligated together into the pEGFP-N2 expression vector digested with SalI and BamH1. The nucleotide sequence of both strands of the new construct (pCX_3CL1-GFP) was determined to verify its identity. ECV-304 cells were grown in Medium 199 (Invitrogen) containing 10% fetal calf serum and transfected by electroporation (Gene Pulser II, Bio-Rad) and selected in 500 μg/ml G418 (Invitrogen). CX_3CL1 expression was determined by flow cytometry. For some experiments ECV-CX_3CL1-GFP cells were grown on glass coverslips and incubated at 37 °C with either colchicine (10 μM) or brefeldin A (100 μM) for 30 min.

COS-7 fibroblast cells were obtained from ATCC and transiently transfected with pCX_3CL1-GFP (COS-CX_3CL1-GFP) using FuGENE (Roche Diagnostics) according to the manufacturer's specifications. Primary porcine aortic endothelial cells (PAEC), a gift from Dr. Aleksander Hinek (The Hospital for Sick Children Research Institute, Toronto, Ontario), were grown in M199 containing 10% fetal calf serum and transfected with the pCX_3CL1-GFP construct by electroporation (PAEC-CX_3CL1-GFP).

Immunofluorescence Staining—ECV-CX_3CL1 cells were grown on glass coverslips, fixed using 4% paraformaldehyde, washed, and blocked with 5% donkey serum at room temperature for 1 h. Cells were incubated with anti-CX_3CL1 antibody (Ab) (2.5 μg/ml) at room temperature for 1 h followed by Alexa 488-conjugated anti-goat IgG. After washing again, the cells were permeabilized using 0.1% Triton. Cells were incubated again with anti-CX_3CL1 Ab, this time followed by Cy3-conjugated anti-goat IgG.

In other experiments ECV-CX_3CL1-GFP or SNARE-transfected ECV-CX_3CL1 cells were grown on glass coverslips, fixed with 4% paraformaldehyde, and permeabilized with 0.1% Triton. Cells were washed and labeled with anti-CX_3CL1 Ab (1 μg/ml) followed by Cy3-conjugated anti-goat IgG. Immunofluorescence was examined using a Leica DMIRE2 microscope and OpenLab software (Improvision Inc., Lexington, MA). Co-localization was determined using OpenLab 4.0.2 co-localization software. The degree of co-localization was expressed using the Pearson's correlation coefficient (r), as previously described (25). In some experiments cells were examined by confocal microscopy using a Zeiss LSM 510 laser scanning confocal microscope with a 100× oil immersion objective and pinhole size 1.00 airy units (26). For some experiments confocal images were deconvolved by importing the LSM file into Volocity 3.0.2 and applying the appropriate point spread function to 95% confidence limit. GFP was examined using conventional laser excitation lines and filter sets.

Quantitation of CX_3CL1 Using Peroxidase-coupled Ab Labeling—To quantify the fraction of CX_3CL1 at the cell surface, cells were grown to confluence in 24-well plates and fixed, and exposed epitopes were saturated by incubating with anti-CX_3CL1 Ab (2.5 μg/ml) at 4 °C for 1 h. To quantify the total amount of CX_3CL1 within the cell, cells were fixed and permeabilized before incubation with anti-CX_3CL1 Ab. Cells were incubated with a blocking solution of 5% donkey serum followed by secondary peroxidase-coupled anti-goat IgG at room temperature for 1 h. Cells were washed, and the reaction was developed using the peroxidase substrate, *o*-phenylenediamine dihydrochloride. The optical density was read by spectrophotometry at 492 nm.

Endocytosis Assays—ECV-CX_3CL1, ECV-CX_3CL1-GFP, COS-CX_3CL1-GFP, or primary PAEC-CX_3CL1-GFP cells were grown on glass coverslips and incubated with anti-CX_3CL1 Ab at 37 or 4 °C for 1 h. Cells were washed, fixed with 4% paraformaldehyde, and permeabilized with 0.1% Triton. Cells were incubated with Cy3-conjugated anti-goat IgG, washed, and mounted on glass slides using DAKO fluorescent mounting medium (DAKO Corp., Carpinteria, CA). In other experiments, after a 1-h serum-free period, ECV-CX_3CL1-GFP cells were incubated with transferrin-rhodamine (30 μg/ml) at 37 °C for 1 h before fixing and mounting. In some experiments, after cells were incubated with anti-CX_3CL1 Ab for 1 h, membrane-associated Ab was removed by acid wash (0.15 M NaCl, 50 mM glycine, 0.1% bovine serum albumin, pH 2.5) on ice using published methods (27). Cells were allowed to recover for various time periods, then washed, fixed, and incubated with Cy3-conjugated secondary Ab. Cell surface immunofluorescence intensity was measured using MetaMorph imaging software (Universal Imaging Corp., Westchester, PA).

Fluorescence Recovery After Photobleaching (FRAP)—Analysis of FRAP was performed as previously described (28, 29). Briefly, ECV-CX_3CL1-GFP or PAEC-CX_3CL1-GFP cells were incubated in medium RPMI containing 10% fetal calf serum and 25 mM HEPES (Invitrogen) and maintained at 37 °C. Live cells were analyzed by confocal microscopy as described above using LP505 filter. A 30-milliwatt LASOS argon laser, set to 25% intensity, was used to irreversibly photobleach a region encompassing the entire CX_3CL1-associated juxtanuclear compartment (≈5-μm diameter). For photobleaching, maximal pinhole size and 100% of set laser intensity were used, whereas 22% intensity was used for image acquisition. The dwell time per pixel was 1.60 μs. The recovery of fluorescence was measured serially over time at 45-s intervals. Control, non-bleached areas of the plasma membrane of the same cell were also serially monitored to quantify the amount of bleaching caused by repeated image acquisition. At the end of each experiment, cells were imaged to ensure that no significant structural or positional changes had occurred during the course of the experiment.

Measurement of pH in the Intracellular CX_3CL1 Compartment—ECV-CX_3CL1 cells were grown on coverslips and incubated for 2 h with anti-CX_3CL1 Ab at 37 °C. Cells were washed then incubated with fluorescein isothiocyanate-conjugated Fab-fragment of anti-goat IgG (20 μg/ml) for 2 h at 37 °C. Coverslips were placed in a Leiden chamber and mounted on the stage of a Leica IRE microscope for ratio determination of emitted fluorescence at 2 excitation wavelengths, 440 and 490 nm, as previously described (30). Excitation filters and image acquisition were controlled using a Lambda 10 filter-wheel controller (Sutter Instrument Company, Novato, CA) driven by the Metafluor software (Universal Imaging, Westchester, PA). A Dell Optiplex DGX 590 computer was interfaced with a Photometrics CCD camera via a 12-bit GPIB/IIA board (National Instruments, Foster City, CA). To generate standard calibration curves of fluorescence ratio *versus* pH, cells were perfused with a series of K^+-rich solutions of known pH, each containing 5 μg/ml nigericin.

RESULTS

The purpose of the initial studies was to examine the subcellular distribution and traffic of CX_3CL1. Endogenous levels of CX_3CL1 in primary cells are difficult to detect using currently available Ab. In light of this, we adopted another approach, namely expressing full-length CX_3CL1 or GFP-tagged CX_3CL1 in ECV-304 cells, a cell line with epithelial and endothelial characteristics (31, 32). In a previous study cell surface levels of CX_3CL1 on CX_3CL1-expressing ECV-304 cells (ECV-CX_3CL1) have been shown to approximate those of primary human vascular endothelial cells, minimizing the risk of mistargeting due to overexpression (9).

CX_3CL1 Is Expressed in Dual Locations within the Cell—ECV-CX_3CL1 cells were fixed and labeled with an Ab directed against the extracellular domain of CX_3CL1. As expected, the Ab labeled only the surface of intact cells, as determined using both conventional epifluorescence (Fig. 1*A*) and confocal mi-

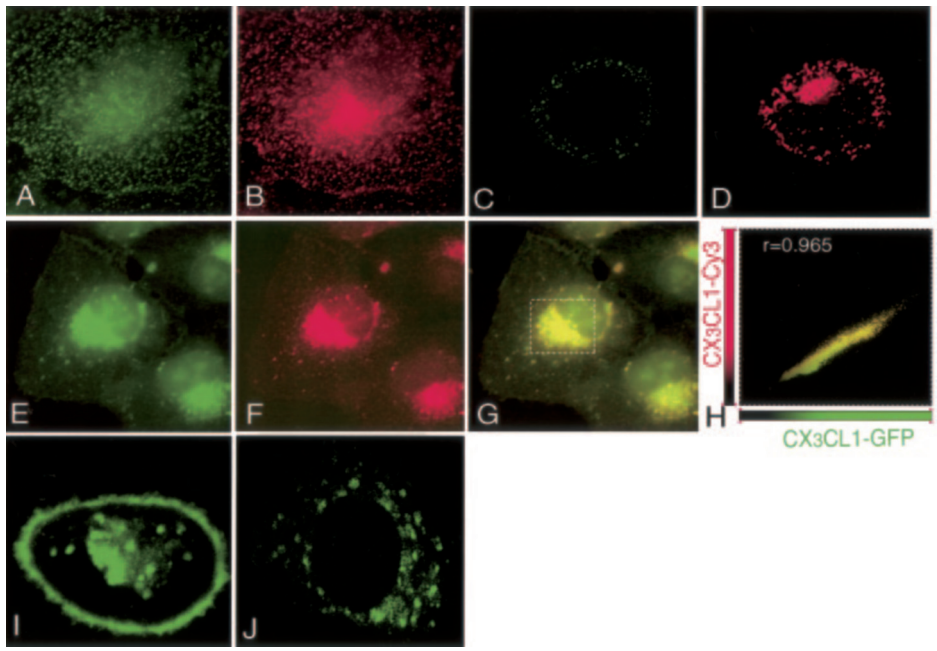

FIG. 1. **CX_3CL1 is expressed in two distinct subcellular locations.** *A*, ECV-CX_3CL1 cells were fixed before labeling with anti-CX_3CL1 Ab and Alexa 488-conjugated secondary Ab. *B*, the same cells were then permeabilized, incubated again with anti-CX_3CL1 Ab, washed, then labeled with Cy3-conjugated secondary Ab. This allowed the separate visualization of intracellular and cell-surface CX_3CL1. *C*, confocal image of cell which was fixed but not permeabilized before labeling with anti-CX_3CL1 Ab. *D*, confocal image of a cell that was both fixed and permeabilized before labeling with anti-CX_3CL1 Ab. *E–H*, ECV-CX_3CL1-GFP cells were fixed, permeabilized, and labeled with anti-CX_3CL1 Ab. The cellular distribution of Ab-labeled CX_3CL1 (*F*) was compared with that of GFP-tagged CX_3CL1 (*E*). *G*, merged image of *E* and *F*. *H*, the degree of overlap of the region indicated by the *dotted line* in *G* was determined using OpenLab 4.0.2 co-localization software and quantitated using the Pearson's correlation coefficient (*r*). *I*, to confirm the existence of separate subcellular and plasma membrane CX_3CL1 expression, cross-sectional images of ECV-CX_3CL1-GFP cells were obtained using confocal microscopy. *J*, to determine whether intracellular CX_3CL1 is associated with microtubules, ECV-CX_3CL1-GFP cells were incubated with colchicine, fixed, and examined by confocal microscopy.

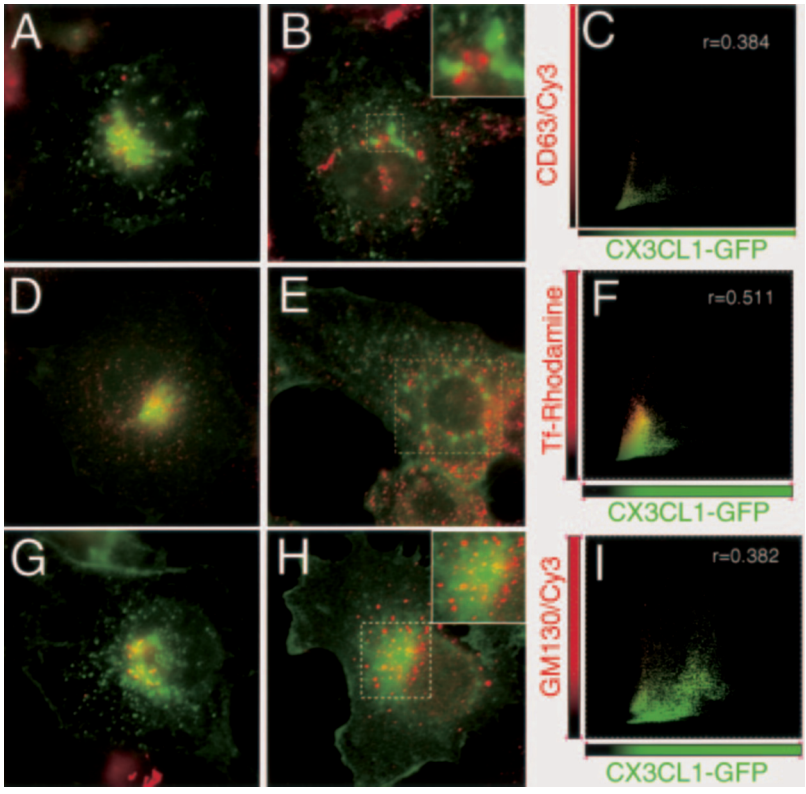

FIG. 2. **Identification of the juxtanuclear CX_3CL1-containing compartment.** ECV-CX_3CL1-GFP cells were fixed, permeabilized, and incubated with Ab recognizing the lysosomal marker CD63 (*A*) or the Golgi marker GM130 (*G*). In other experiments cells were incubated with transferrin-rhodamine at 37 °C for 1 h (*D*). In parallel experiments cells were treated with colchicine before incubation with anti-CD63 Ab (*B*) or transferrin-rhodamine (*E*). *H*, cells were treated with brefeldin A before labeling with anti-GM130 Ab. *C*, *F*, and *I*, the degree of co-localization within the regions indicated by the *dotted lines* in *B*, *E*, and *H* was determined using OpenLab 4.0.2 co-localization software (*C*, co-localization between CX_3CL1-GFP and CD63/Cy3; *F*, co-localization between CX_3CL1-GFP and transferrin-rhodamine; *I*, co-localization between CX_3CL1-GFP and GM130/Cy3). *Large panel insets* in *B* and *H* represent a magnified view of the areas indicated by the *dotted lines*.

croscopy (Fig. 1*C*). To assess whether CX_3CL1 is also present intracellularly, the same cells were then permeabilized and labeled again with anti-CX_3CL1 Ab followed by incubation with a different secondary Ab. Permeabilization revealed a sizable intracellular pool of CX_3CL1 with juxtanuclear location (epifluorescence microscopy, Fig. 1*B*; confocal microscopy, Fig. 1*D*). The relative magnitude of the surface and endomembrane compartments was quantified using a spectroscopic immunoperoxidase labeling method (see "Experimental Procedures"). The plasmalemmal component of CX_3CL1 was found to account for

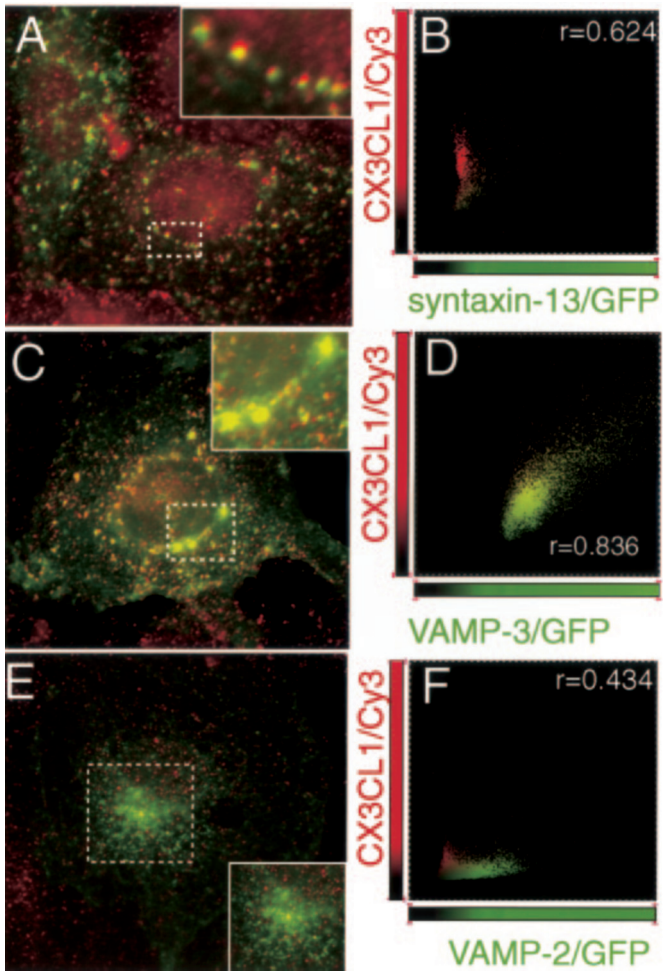

FIG. 3. **Co-localization of intracellular CX_3CL1 with SNARE proteins implicated in recycling of plasma membrane proteins.** ECV-CX_3CL1 cells were transfected with cDNA for GFP-tagged syntaxin-13 (*A* and *B*), VAMP-3 (*C* and *D*), or VAMP-2 (*E* and *F*). To obviate any fortuitous overlap, cells were also treated with colchicine then fixed, permeabilized, and labeled with anti-CX_3CL1 Ab and Cy3-conjugated secondary Ab. The distribution of each GFP-tagged SNARE protein was compared with that of CX_3CL1 in the same cell (*A* and *B*, syntaxin-13; *C* and *D*, VAMP-3; *E* and *F*, VAMP-2). The degree of co-localization within the regions indicated by the *dotted lines* in *A*, *C*, and *E* was determined using OpenLab 4.0.2 co-localization software (*B*, co-localization between CX_3CL1/Cy3 and syntaxin-13/GFP; D, co-localization between CX_3CL1/Cy3 and VAMP-3-GFP; *F*, co-localization between CX_3CL1/Cy3 and VAMP-2/GFP). *Large panel insets* in *A* and *C* and *E* represent a magnified view of the areas indicated by the *dotted lines*.

57 ± 6% of the total cellular pool of CX_3CL1.

The existence of CX_3CL1 in at least two distinct cellular compartments was verified in cells expressing GFP-tagged CX_3CL1 (ECV-CX_3CL1-GFP). In this construct GFP is attached to the cytosolic tail of the transmembrane chemokine. The fact that the tagged construct (Fig. 1*E*) was recognized by the antibody directed to the extracellular domain anti-CX_3CL1 Ab (Fig. 1*F*) confirms that the expressed protein traverses the membrane. The presence of GFP and antibody fluorescence at the surface and in the juxtanuclear endomembrane vesicles implies that the full-length transmembrane protein is found in both locations (Fig. 1, *G* and *H*). The similarity of this distribution to that of the untagged protein indicates that linkage to GFP did not visibly alter the cellular targeting of CX_3CL1.

We also used confocal microscopy to verify that GFP-tagged CX_3CL1 is indeed expressed in dual locations. As shown in Fig. 1*I*, cross-sectional analysis confirmed that CX_3CL1-GFP is expressed not only in the plasma membrane but also within a juxtanuclear compartment. The endomembrane compartment appears to be maintained in its juxtanuclear location by microtubules, since treatment with colchicine caused the intracellular CX_3CL1-GFP to disperse (Fig. 1*J*). Interestingly, treatment with colchicine also caused an appreciable decrease in plasma membrane CX_3CL1-GFP signal. These data raise the possibility that cell surface CX_3CL1 is in dynamic exchange with the pool of intracellular CX_3CL1 and that this exchange relies on intact microtubules.

Identification of the Juxtanuclear CX_3CL1-associated Compartment—The identity and function of the intracellular CX_3CL1 compartment were investigated next. We initially assessed whether CX_3CL1 was located in lysosomes, recycling endosomes, or the Golgi apparatus, all of which are maintained in a juxtanuclear position by retrograde transport along microtubules. ECV-CX_3CL1-GFP cells were labeled with a late endosomal/lysosomal marker, anti-CD63 Ab (Fig. 2*A*). As expected, some degree of co-localization was detected in the juxtanuclear region. To obviate the possibility that overlap was fortuitous, due to the presence of multiple organelles in the same general region, cells were treated with colchicine before staining (Fig. 2*B*). Under these conditions no significant degree of association between CD63 and the CX_3CL1-containing vesicles was observed (Fig. 2, *B* and *C*; Pearson's colocalization coefficient $r = 0.317 \pm 0.041$; $p > 0.1$), demonstrating that the latter compartment does not correspond to late endosomes/lysosomes.

To investigate whether the intracellular CX_3CL1 compartment is associated with recycling endosomes, ECV-CX_3CL1-GFP cells were incubated with rhodamine-conjugated transferrin for 1 h at 37 °C with (Fig. 2*E*) or without (Fig. 2*D*) colchicine treatment. As shown in Fig. 2*D*, transferrin was indeed internalized to a juxtanuclear location resembling that of CX_3CL1. However, when the organelles were dispersed by microtubule disruption, only partial overlap was observed (Fig. 2, *E* and *F*), yielding Pearson's correlation coefficient slightly greater than 0.5, which is statistically significant ($r = 0.515 \pm 0.071$; $p < 0.05$) and indicative of partial colocalization. Thus, the intracellular CX_3CL1-containing compartment overlaps with but is not entirely identical to the transferrin receptor-containing recycling endosomes.

In similar experiments CX_3CL1-containing vesicles were found to be distinct from the Golgi stacks, identified using anti-GM130 Ab (Fig. 2, *G–I*). A dissociation between the two compartments was also noted when the cells were pretreated with brefeldin (Fig. 2*H*; $r = 0.322 \pm 0.068$; $p > 0.1$), which is known to disperse the Golgi cisternae while compacting both recycling endosomes and the *trans*-Golgi network. A sizable fraction of CX_3CL1 remained compacted near the nucleus, consistent with location in recycling endosomes and/or *trans*-Golgi network. Collectively, these data demonstrate that CX_3CL1 is expressed within a specialized juxtanuclear compartment that is distinct from late endosomes/lysosomes and Golgi cisternae but which partially co-localizes with transferrin receptor-associated recycling endosomes.

SNARE Proteins in the Intracellular CX_3CL1 Compartment—To further characterize the intracellular CX_3CL1 compartment and to investigate its possible relationship with the plasmalemmal pool, we proceeded to study molecular entities that might mediate fusion of CX_3CL1-bearing vesicles with the plasma membrane. The SNARE family of proteins is thought to mediate the docking and fusion of vesicles with their target membranes, thereby facilitating the delivery of cargo between compartments. In an attempt to identify SNARE proteins, ECV-CX_3CL1 cells were transiently transfected with DNA con-

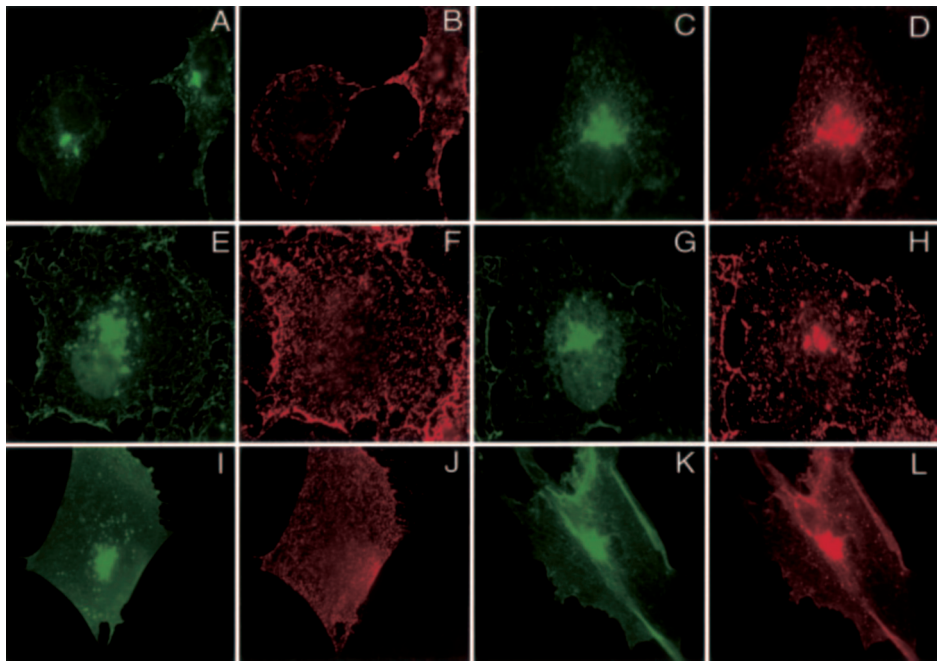

FIG. 4. **Cell surface CX_3CL1 is internalized in diverse cell types.** *A* and *B*, at 4 °C, ECV-CX_3CL1-GFP cells were incubated with anti-CX_3CL1 Ab, then fixed, permeabilized, and incubated with Cy3-conjugated secondary Ab. Because recycling cannot occur at 4 °C, anti-CX_3CL1 Ab labeled only the surface of cells (*B*) but not the internal CX_3CL1-GFP-containing compartment (*A*). *C* and *D*, similar experiments were performed at 37 °C to allow endocytosis to occur. At 37 °C Ab-labeled CX_3CL1 was internalized (*D*) and co-localized with the internal CX_3CL1-GFP-containing compartment (*C*). *E–H*, to confirm that endocytosis of plasma membrane CX_3CL1 was not unique to ECV-304 cells, similar experiments were performed using GFP-tagged CX_3CL1-expressing COS-7 fibroblasts (COS-CX_3CL1-GFP). At 4 °C, anti-CX_3CL1 Ab labeled only the surface of cells (*F*) but not the internal CX_3CL1-GFP-containing compartment (*E*). At 37 °C, Ab-labeled CX_3CL1 was internalized (*H*) and co-localized with the internal CX_3CL1-GFP-containing compartment (*G*). *I–L*, similar experiments were conducted using primary porcine aortic endothelial cells that expressed GFP-tagged CX_3CL1 (PAEC-CX_3CL1-GFP). At 4 °C, anti-CX_3CL1 Ab labeled only the surface of PAEC-CX_3CL1-GFP (*J*) but not the internal CX_3CL1-GFP-containing compartment (*I*). At 37 °C, Ab-bound CX_3CL1 was internalized (*L*) and co-localized with the internal CX_3CL1-GFP-containing compartment (*K*).

structs encoding VAMP-2-GFP, VAMP-3-GFP, or syntaxin-13-GFP, which are known components of the endocytic and recycling pathway. Cells were fixed, permeabilized, and immunostained with anti-CX_3CL1 Ab to determine possible co-localization. As before, fortuitous overlap was minimized by pretreating the cells with colchicine. As illustrated in Fig. 3, the intracellular CX_3CL1 compartment partially co-localized with syntaxin-13 (Fig. 3, *A* and *B*; $r = 0.632 \pm 0.032$; $p < 0.01$) as well as with VAMP-3 (Fig. 3, *C* and *D*; $r = 0.793 \pm 0.009$; $p < 0.01$). No significant co-localization with VAMP-2 was observed (Fig. 3, *E* and *F*; $r = 0.395 \pm 0.033$; $p > 0.1$). These data support the notion that intracellular CX_3CL1 represents a subcompartment of recycling endosomes and suggest that recycling may occur by SNARE-mediated fusion of endosomal and plasmalemmal membranes.

Plasma Membrane CX_3CL1 Undergoes Endocytosis in Diverse Cell Types—To ensure that the dual localization of CX_3CL1 is not an idiosyncratic feature of ECV-304 cells, we transfected the tagged CX_3CL1 in other cell types known to express the chemokine, namely primary porcine aortic endothelial cells and fibroblastic cells (COS-7). In both of these cell types, CX_3CL1 was expressed with a distribution similar to that seen in ECV cells, namely, on the plasma membrane as well as in an intracellular location (see Fig. 4).

The results from the preceding experiments suggested that intracellular CX_3CL1 may represent a recycling endosomal pool. To verify this prediction, we incubated ECV-CX_3CL1-GFP, COS-CX_3CL1-GFP, and PAEC-CX_3CL1-GFP cells with an Ab directed to the exofacial domain of CX_3CL1 for 2 h at 37 °C. The cells were washed, fixed, and permeabilized before incubating with secondary Ab. In all three cell types tagged CX_3CL1 was seen to accumulate in the juxtanuclear location in a time-dependent fashion (Fig. 4, *C*, *D*, *G*, *H*, *K*, and *L*), providing evidence of dynamic exchange between compartments. Labeling of the juxtanuclear pool was prevented when the experiment was performed at 4 °C. In this instance only the superficial CX_3CL1 was labeled (Fig. 4, *A*, *B*, *E*, *F*, *I*, and *J*), implying that endocytosis is required to deliver the antibody to the intracellular pool.

Recovery of Fluorescence after Photobleaching of the CX_3CL1-containing Juxtanuclear Compartment—Because Fab fragments of anti-CX_3CL1 are not available, the preceding experiments utilized bivalent antibodies to tag CX_3CL1. It is, therefore, conceivable that the observed internalization is not a constitutive phenomenon but was instead induced by cross-linking caused by the antibodies. Indeed, traffic of several proteins is known to be altered by their clustering.

To circumvent this problem, we used a second, complementary approach, based on FRAP. We took advantage of the fluorescence of the CX_3CL1-GFP chimera to monitor the replenishment of the juxtanuclear pool after elimination of its fluorescence by photobleaching. Briefly, a region near the center of the cell (≈ 5 μm diameter) encompassing the entire juxtanuclear CX_3CL1-GFP compartment was irreversibly photobleached using an intense laser beam, and the recovery of fluorescence was monitored over time (Fig. 5, *A–C*). The fluorescence of the plasma membrane pool, which remained largely unaffected by the bleaching procedure, was also monitored. Fig. 5*A* depicts an ECV-CX_3CL1-GFP cell before bleaching, and Fig. 5, *B* and *C*, illustrate the same cell immediately after and 5 min after bleaching, respectively. Note that the plasmalemmal fluorescence decreased as the juxtanuclear fluorescence recovered, consistent with delivery of unbleached CX_3CL1-GFP from the former to the latter compartment. The rate of recovery of endomembrane fluorescence was quantified, and a typical experiment is illustrated in Fig. 5*D*. In four similar experiments,

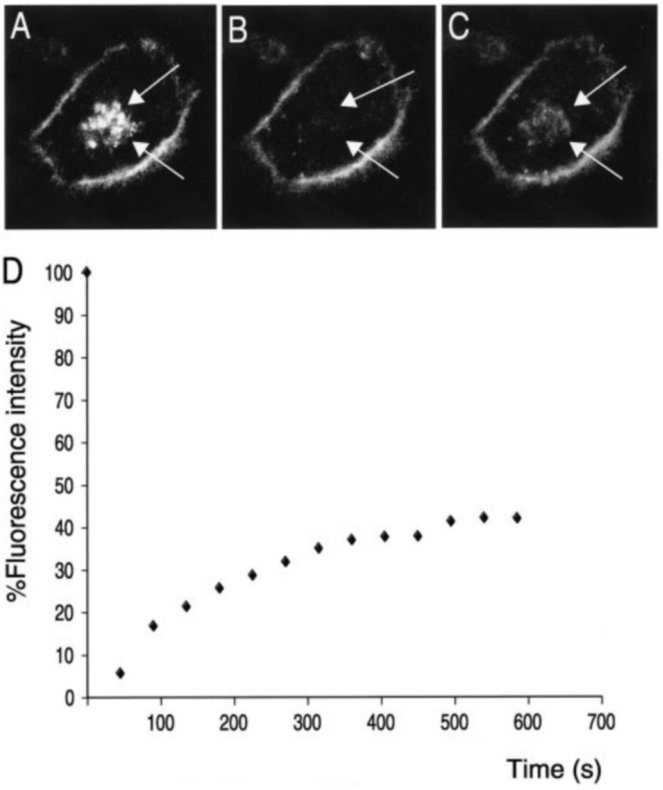

FIG. 5. **CX_3CL1 is internalized from the cell surface.** To confirm that cell surface CX_3CL1 recycles, FRAP was performed as described under "Experimental Procedures." Using an argon laser and a scanning confocal microscope, the juxtanuclear CX_3CL1-containing compartment was irreversibly photobleached (*arrows*), and recovery of fluorescence was determined at 45-s intervals. *A* represents ECV-CX_3CL1-GFP cell before bleaching, *B* depicts the same cell immediately after photobleaching, and *C* depicts the cell 5 min later. Control areas of the same diameter in the plasma membrane were examined at each time point. *D*, at each time point the ratio of the fluorescence intensity of the internal compartment to the mean control membrane fluorescence intensity was calculated. Recovery of fluorescence intensity of the juxtanuclear compartment for 1 of 4 similar experiments.

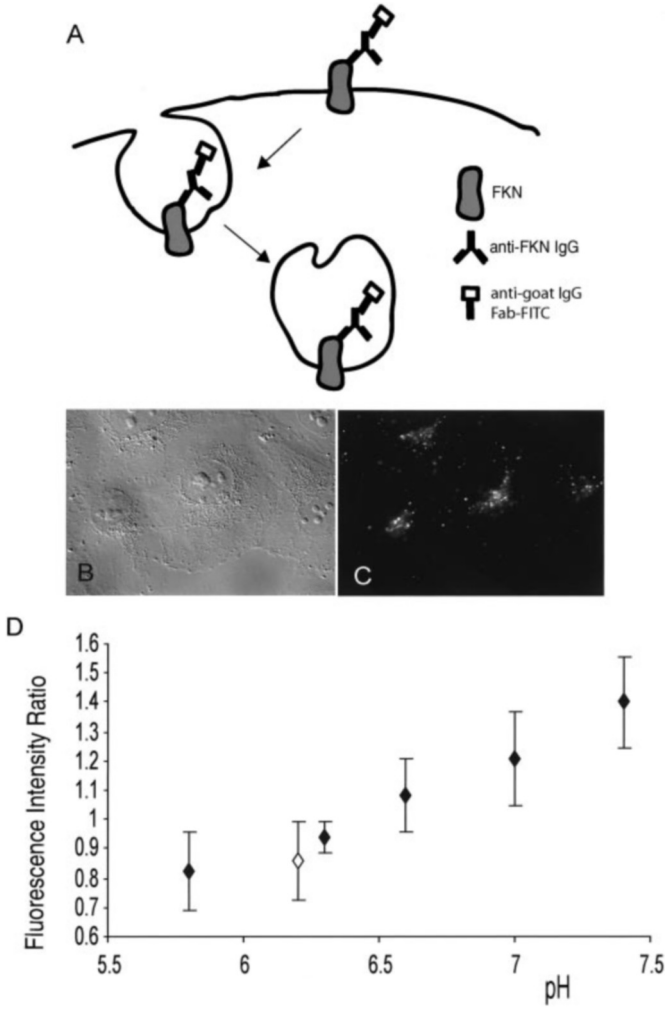

FIG. 6. **The juxtanuclear CX_3CL1-containing compartment is moderately acidic.** *A*, ECV-CX_3CL1 cells were grown on coverslips and incubated with anti-CX_3CL1 Ab and a fluorescein isothiocyanate (*FITC*)-conjugated Fab fragment of anti-goat IgG at 37 °C, as described under "Experimental Procedures." Shown are a Nomarski image (*B*) and immunofluorescent image (*C*) of cells labeled as described. The ratio of emitted fluorescence at excitation wavelengths 440 and 490 nm was determined and compared with standard calibration curves, as described under "Experimental Procedures." *D*, standard curve (*closed diamonds*) and juxtanuclear CX_3CL1 fluorescence intensity ratio (*open diamonds*) for the average of four experiments. *FKN*, fractalkine.

the juxtanuclear CX_3CL1-GFP compartment recovered 44 ± 9% of its original fluorescence, with half-maximal recovery occurring by 208 ± 72 s. These experiments confirm the existence of a constitutive recycling of CX_3CL1 between the surface and internal compartments, with a half-life of ~3.5 min. To further confirm the ability of CX_3CL1 to recycle in primary vascular endothelial cells, we examined FRAP after photobleaching the juxtanuclear compartment in PAEC-CX_3CL1-GFP. In 6 similar experiments, the juxtanuclear CX_3CL1-GFP compartment recovered 43 ± 5% of its original fluorescence, with half-maximal recovery occurring by 78 ± 2 s (data not shown). These data demonstrate that CX_3CL1 recycles not only in transformed cell lines but also in primary vascular endothelial cells.

The Intracellular CX_3CL1-associated Compartment Is Moderately Acidic—Different subcompartments of the endocytic and secretory pathways have distinctive luminal pH values (30, 33–35). To better characterize the internal CX_3CL1 compartment, we measured its internal pH. The ability of CX_3CL1 to continuously cycle between the surface and internal compartments (see "Results") was harnessed to label the endomembrane CX_3CL1 compartment with a pH-sensitive fluorescent probe, as illustrated by the diagram in Fig. 6*A*. An antibody directed to the exofacial domain of CX_3CL1 was tagged with a fluorescein isothiocyanate-conjugated Fab fragment and allowed to bind to the plasmalemmal chemokine. Over time, tagged CX_3CL1 accumulated in the juxtanuclear location (Fig. 6, *B* and *C*). The ratio of emitted fluorescence when cells were excited at 440 and 490 nm was measured to provide a concentration- and photobleaching-independent measure of compartmental pH. Absolute pH values were obtained by comparison to an internal standard calibration curve (Fig. 6*D*), obtained *in situ* using ionophores. The mean pH of the intracellular CX_3CL1 compartment was found to be 6.3 ± 0.2. This moderately acidic pH is similar to that of recycling endosomes (30) and differs from the neutral pH of the endoplasmic reticulum and the much more acidic pH of lysosomes and secretory granules (30, 33, 35, 36).

Internalized CX_3CL1 Cycles Back to the Plasma Membrane—The preceding experiments show that CX_3CL1 can translocate from the plasmalemma to the endomembrane compartment. At steady state, one would predict that an equivalent exocytic delivery of the chemokine would exist to maintain a constant amount of CX_3CL1 at the surface. To validate this notion, the endomembrane pool was first loaded by incubation with anti-CX_3CL1 Ab at 37 °C for 1 h. Bound Ab remaining at the cell surface was then acutely removed by briefly stripping with an

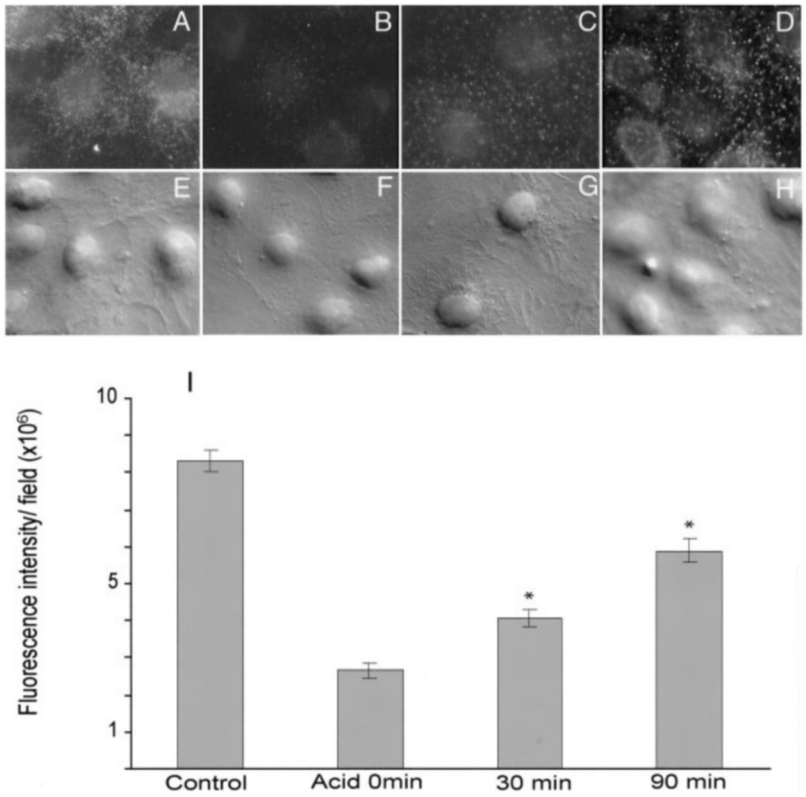

FIG. 7. **Internalized CX_3CL1 traffics back to the plasma membrane.** ECV-CX_3CL1 cells were incubated with anti-CX_3CL1 Ab at 37 °C for 1 h, then membrane-associated Ab was removed by acid wash (pH 2.5) at 4 °C. Cells were allowed to recover for the indicated time period, then washed, fixed, and incubated with Cy3-conjugated secondary Ab. Shown are an immunofluorescent image of membrane-associated anti-CX_3CL1 Ab labeling (*A*) and Nomarski image (*E*) of cells before acid-stripping. Shown are an immunofluorescent image of membrane-associated anti-CX_3CL1 Ab labeling (*B*) and Nomarski image (*F*) of cells immediately after acid-stripping. Also shown are an immunofluorescent image (*C*) and Nomarski image (*G*) of cells 30 min after recovering from acid shock. An immunofluorescent image (*D*) and Nomarski image of cells (*H*) 90 min after recovering from acid shock is shown. *I*, cell surface immunofluorescence was quantitated using MetaMorph Imaging Software. Results represent mean values of 64–72 fields per treatment condition. *, $p < 0.0001$ *versus* acid at 0 min.

acidic solution. The cells were then incubated further, and the reinsertion of CX_3CL1 in the plasma membrane was followed by quantifying the reappearance of the antibody, labeling with a secondary Ab, and quantifying cell surface immunofluorescence. As shown in Fig. 7, fluorescence at the surface increased progressively after acid stripping, confirming the occurrence of exocytosis of CX_3CL1 from the endomembrane compartment. Thus, the chemokine indeed recycles actively between the superficial and internal compartments.

Functional Inhibition of VAMP-3 and Syntaxin-13 Inhibits Cycling of Internalized CX_3CL1 Back to the Plasma Membrane—Because intracellular CX_3CL1 co-localizes with SNARE proteins known to mediate recycling, we next sought to determine whether functional inhibition of such proteins would alter traffic of CX_3CL1. To this end, ECV-CX_3CL1 cells were transfected with either mammalian tetanus toxin, known to selectively cleave VAMP-3 and thereby inhibit its function, or with a dominant negative allele of syntaxin-13 (syntaxin-13-DN). In each case, cells were co-transfected with EGFP to allow identification of transfected cells. Exocytic delivery of CX_3CL1 was determined using the pre-loading and acid-stripping protocol described above. Cells were allowed to recover for various time periods then fixed and incubated with a Cy3-conjugated secondary Ab for quantitation of CX_3CL1 delivery to the surface. As illustrated in Fig. 8, *A–F*, recycling of internalized CX_3CL1 to the surface of the cells was severely impaired by tetanus toxin as well as by the dominant negative truncated form of syntaxin-13 compared with cells transfected with only EGFP. For cells transfected with EGFP alone, cell surface fluorescence intensity recovered from 25 ± 1 to 57 ± 5 by 30 min. In comparison, for cells expressing syntaxin-13-DN, fluorescence intensity recovered from 31 ± 2 to 35 ± 1. Surface fluorescence intensity of cells transfected with tetanus toxin recovered from 31 ± 1 to 37 ± 2. Overall, in four experiments dominant negative syntaxin-13 depressed recycling by 86%, whereas tetanus toxin effected a 82% decrease (Fig. 8*G*).

DISCUSSION

The principal aim of this study was to investigate the subcellular distribution and traffic of CX_3CL1 within cells. For some of these experiments we used ECV-304 cells transfected with either untagged or GFP-conjugated CX_3CL1. ECV-304 cells were initially described as a spontaneously immortalized derivative of human endothelial cells (37). Indeed, ECV-304 cells retain several endothelial characteristics, including the tendency to grow as monolayers of flattened cells, typical of endothelium (37–39), and expression of the endothelial markers Flt-1 and von Willebrand factor (40, 41). However, more recently it has become apparent that the ECV-304 line is in fact derived from cancerous bladder epithelial cells and is closely related to the T-24 line (40, 41). Accordingly, ECV-304 cells grown in monolayers target E-cadherin to the basolateral surface and hemagglutinin from influenza virus to the apical surface (32) and separate these domains by junctions with reduced permeability to inulin. Yet, these junctions are not as "tight" as those seen in other epithelial monolayers (32). Thus, it appears that ECV-304 cells have a phenotype that is intermediate between endothelial and epithelial cells. In any event, they are a useful model to study cellular CX_3CL1 distribution and traffic inasmuch as this chemokine is endogenously expressed by both endothelial and epithelial cells (4, 9, 14, 42). To ensure that the observed trafficking of CX_3CL1 was not an idiosyncratic feature of transfected ECV-304 cells, we further confirmed our findings in other cell types known to express CX_3CL1, namely fibroblasts (43) and, especially, primary arterial endothelial cells (5, 6, 9, 12, 44).

CX_3CL1 is synthesized as a 50–75-kDa precursor that is rapidly processed, presumably glycosylated, yielding the mature 100-kDa species (45). The mature form can be cleaved from the cell surface to yield a soluble 85-kDa fragment encompassing the majority of the ectodomain (45). Cleavage of CX_3CL1 proceeds both constitutively and inducibly. Constitutive cleavage occurs at low levels and is mediated by the met-

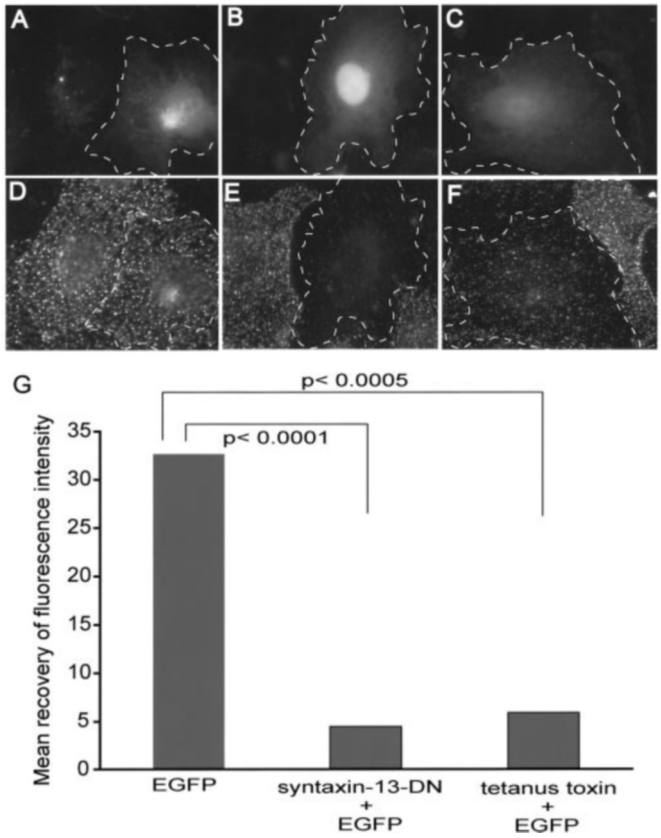

FIG. 8. **Functional inhibition of syntaxin-13 and VAMP-3 inhibits cycling of internalized CX_3CL1 back to the plasma membrane.** *A–F*, ECV-CX_3CL1 cells were transfected with EGFP alone (*A* and *D*), a dominant negative allele of syntaxin-13 (syntaxin-13-DN; *B* and *E*), or with mammalian tetanus toxin (*C* and *F*). Cells transfected with the syntaxin-13-DN and mammalian tetanus toxin constructs were co-transfected with EGFP at 1:10 to allow identification of transfected cells (*dotted lines*). Exocytic delivery of CX_3CL1 was determined using the preloading and acid-stripping protocol described above. Cells were allowed to recover for 0 or 30 min, then fixed and incubated with a Cy3-conjugated secondary Ab for quantitation of CX_3CL1 delivery to the surface. The *dotted line* in *D* depicts cell surface fluorescence intensity of EGFP-transfected cell indicated in *A* after a 30-min recovery period after acid stripping. The *dotted line* in *E* depicts cell surface fluorescence intensity of syntaxin-13-DN/EGFP-expressing cell indicated in *B* after a 30-min recovery period. The *dotted line* in *F* depicts cell surface fluorescence intensity of tetanus toxin/EGFP-transfected cell indicated in *C* after a 30-min recovery period. *G*, the mean surface fluorescence intensity of 50 transfected cells per treatment group was quantitated using MetaMorph Imaging Software by determining the average pixel number per unit area. The mean recovery of fluorescence intensity after 30 min was, thus, calculated for 4 separate experiments.

alloprotease, ADAM-10 (46). Through the actions of the protease, tumor necrosis factor-converting enzyme (TACE) (45, 47), CX_3CL1 can be rapidly shed from the cell surface after cell stimulation with inflammatory agents such as LPS, IL-1β or phorbol esters (13, 45, 47). Knowledge regarding these proteolytic events is fairly rudimentary. In particular, the subcellular distribution and mode of activation of TACE and the location of CX_3CL1 at the time of degradation are not well characterized.

A major finding of this study is that CX_3CL1 is expressed in dual locations within the cell; at the plasma membrane as well as in an intracellular compartment. This pattern of expression was observed in several cell types, including CX_3CL1-expressing ECV-304 cells, COS-7 fibroblasts, and primary porcine aortic endothelial cells. We were further able to demonstrate that plasma membrane CX_3CL1 actively recycles between these two compartments. The endomembrane compartment where CX_3CL1 resides appears to share some features with early/recycling endosomes, but the two compartments are not identical. Thus, the endosomal markers VAMP-3 and syntaxin-13 showed significant co-localization with CX_3CL1. Moreover, the compartment occupied by CX_3CL1 was determined to have a luminal pH of 6.3, similar to that of early/recycling endosomes (30). Last, the CX_3CL1 compartment collapsed near the nucleus upon addition of brefeldin A, as is known to be the case for recycling endosomes.

In our studies the overlap of CX_3CL1 with transferrin receptors was imperfect, suggesting that they only partially occupy a common compartment. These data are consistent with reports in the literature that support the existence of distinct subcompartments within the recycling vesicular pool and with the fact that transferrin receptors are also found elsewhere. Internalized transferrin accumulates within early endosomes containing early endosomal antigen 1 (48) and the small GTPase, Rab4 (49, 50). With time, transferrin accumulates within a second endosomal fraction that is devoid of Rab4 (49) and endosomal antigen 1 but which contains Rab11 (48). Recent studies have further clarified the role of Rab11 in protein recycling. Unlike Rab4, Rab11-containing vesicles can associate with the Sec15 exocyst subunit and fuse with the plasma membrane in exocytosis (51, 52). In our studies a significant portion of CX_3CL1 did not co-localize with transferrin receptor. It is conceivable that CX_3CL1 resides in a distinct, specialized recycling subcompartment, as has been described for the GLUT-4 glucose transporters and for proton pumps in certain specialized tissues (53–56).

Our studies also provide initial information of the molecular mechanisms involved in CX_3CL1 recycling. The functional implication of VAMP-3 and syntaxin-13 in recycling of CX_3CL1 may serve in future studies to modulate the biological effects of the chemokine.

Recycling of CX_3CL1 was found to occur constitutively in unstimulated cells, including both immortalized cell lines and primary endothelial cells. The significance of this basal recycling is not clear, but it may serve to expose CX_3CL1 to a subpopulation of TACE. In a recent study, endogenous TACE in COS-7 cells was reported to localize predominantly in a perinuclear location, with smaller amounts found at the cell surface and in the endoplasmic reticulum (57). It is, therefore, possible that a fraction of the cleavage of CX_3CL1 occurs intracellularly. In this regard delivery of CX_3CL1 to an acidic endomembrane compartment may facilitate its fragmentation, since TACE is known to be synthesized as a proenzyme that is subsequently activated by furin or a furin-like enzyme (57). Of note, furin and the related prohormone convertase PC1 have optimal catalytic activity in moderately acidic environments (58–60) like that prevailing in the lumen of the recycling endosomes and *trans*-Golgi network, where they reside.

It is also possible that the rate of basal recycling of CX_3CL1 can be regulated. By accelerating exocytosis, stimuli may mobilize the intracellular storage depot to enhance chemoattractant release and/or replenish the chemokine associated with the cell surface. Conversely, stimulation of endocytosis may represent a means of down-regulating CX_3CL1 at the cell surface, with relocation to an internal storage site. The balance between the net rates of endocytosis and exocytosis coupled with the rate of cleavage of CX_3CL1 from the plasma membrane would collectively determine the net exposure of CX_3CL1 at the cell surface. Of interest, regulated recycling of membrane proteins located in specialized recycling compartments, such as aquaporin-2 and GLUT-4, is key to controlling their function. Thus, regulation of water reabsorption in the kidney and of glucose uptake by adipocytes and myocytes depends critically on membrane traffic (61–63). Further work will be needed to ascertain if and how inflammatory stimuli influence the spontaneous rate of CX_3CL1 recycling.

In summary, we have identified a distinct storage compartment for CX_3CL1. Unlike the surface component of CX_3CL1, which functions as a tethering site or a source of chemoattractant for leukocytes bearing CX_3CR1 receptors, the subcellular compartment may serve as the source for acute up-regulation of levels of surface CX_3CL1. Modulation of the rates of CX_3CL1 endocytosis and/or exocytosis could, therefore, provide an alternate means of regulation of chemokine abundance and accessibility independent of *de novo* biosynthesis.

Acknowledgments—We thank Dr. Bill Trimble for providing DNA constructs as well as Cameron Scott, Mauricio Terebiznik, and Elaine Corbett for expert technical and computer assistance. We are indebted to Dr. Sergio Grinstein for many helpful discussions and critical review of the manuscript.

REFERENCES

1. Olson, T., and Ley, K. (2002) *Am. J. Physiol. Regul. Integr. Comp. Physiol.* **283,** 7–28
2. Feng, L., Chen, S., Garcia, G., Xia, Y., Siani, M., Botti, P., Wilson, C., Harrison, J., and Bacon, K. (1999) *Kidney Int.* **56,** 612–620
3. Haskell, C., Hancock, W., Salant, D., Gao, W., Csizmadia, V., and Peters, W. (2001) *J. Clin. Investig.* **108,** 679–688
4. Robinson, L., Nataraj, C., Thomas, D., Howell, D., Griffiths, R., Bautch, V., Patel, D., Feng, L., and Coffman, T. (2000) *J. Immunol.* **165,** 6067–6072
5. Combadiere, C., Potteaux, S., Gao, J., Esposito, B., Casanova, S., Lee, E., Debre, P., Tedgui, A., Murphy, P., and Mallat, Z. (2003) *Circulation* **107,** 1009–1016
6. Lesnik, P., Haskell, C., and Charo, I. (2003) *J. Clin. Investig.* **111,** 333–340
7. Bazan, J., Bacon, K., Hardiman, G., Wang, W., Soo, K., Rossi, D., Greaves, D., Zlotnick, A., and Schall, T. (1997) *Nature* **385,** 640–644
8. Imai, T., Hieshima, K., Haskell, C., Baba, M., Nagira, M., Nishimura, M., Kakizaki, M., Takagi, S., Nomiyama, H., Schall, T., and Yoshie, O. (1997) *Cell* **91,** 521–530
9. Fong, A., Robinson, L., Steeber, D., Tedder, T., Yoshie, O., Imai, T., and Patel, D. (1998) *J. Exp. Med.* **188,** 1413–1419
10. Fong, A., Erickson, H., Zachariah, J., Poon, S., Schamberg, N., Imai, T., and Patel, D. (2000) *J. Biol. Chem.* **275,** 3781–3786
11. Kerfoot, S., Lord, S., Bell, R., Gill, V., Robbins, S., and Kubes, P. (2003) *Eur. J. Immunol.* **33,** 729–739
12. Harrison, J., Jiang, Y., Wees, E., Salafranca, M., Liang, H., Feng, L., and Belardinelli, L. (1999) *J. Leukocyte Biol.* **66,** 937–944
13. Ludwig, A., Berkhout, T., Moores, K., Groot, P., and Chapman, G. (2002) *J. Immunol.* **168,** 604–612
14. Muehlhoefer, A., Saubermann, L., Gu, X., Luedtke-Heckenkamp, K., Xavier, R., Blumberg, R., Podolsky, D., MacDermott, R., and Reinecker, H. (2000) *J. Immunol.* **164,** 3368–3376
15. Brown, D. (2003) *Am. J. Physiol. Renal Physiol.* **284,** 893–901
16. Gentzsch, M., Chang, X., Cui, L., Wu, Y., Ozols, V., Choudhury, A., Pagano, R., and Riordan, J. (2004) *Mol. Biol. Cell* **15,** 2684–2696
17. Liu, L., Omata, W., Kojima, I., and Shibata, H. (2003) *J. Biol. Chem.* **278,** 30157–30169
18. Sharma, M., Pampinella, F., Nemes, C., Benharouga, M., So, J., Du, K., Bache, K., Papsin, B., Zerangue, N., Stenmark, H., and Lukacs, G. (2004) *J. Cell Biol.* **164,** 923–933
19. Zeigerer, A., Lampson, M., Karylowski, O., Sabatini, D., Adesnik, M., Ren, M., and McGraw, T. (2002) *Mol. Biol. Cell* **13,** 2421–2435
20. Advani, R., Bae, H.-R., Bock, J., Chao, D., Doung, Y.-C., Prekeris, R., Yoo, J.-S., and Scheller, R. (1998) *J. Biol. Chem.* **273,** 10317–10324
21. Chao, D., Hay, J., Winnick, S., Prekeris, R., Klumperman, J., and Scheller, R. (1999) *J. Cell Biol.* **144,** 869–881
22. Collins, R., Schreiber, A., Grinstein, S., and Trimble, W. (2002) *J. Immunol.* **169,** 3250–3256
23. Huang, X., Kang, Y., Pasyk, E., Sheu, L., Wheeler, M., Trimble, W., Salapatek, A., and Gaisano, H. (2001) *Am. J. Physiol. Cell Physiol.* **281,** 740–750
24. Randhawa, V., Bilan, P., Khayat, Z., Daneman, N., Liu, Z., Ramlal, T., Volchuk, A., Peng, X., Coppola, T., Regazzi, R., Trimble, W., and Klip, A. (2000) *Mol. Biol. Cell* **11,** 2403–2417
25. Manders, M., Verbeek, F., and Aten, J. (1993) *J. Microsc.* (*Oxf.*) **169,** 375–382
26. Terebiznik, M., Vieira, O., Marcus, S., Slade, A., Yip, C., Trimble, W., Meyer, T., Finlay, B., and Grinstein, S. (2002) *Nat. Cell Biol.* **4,** 766–773
27. van Kerkhof, P., Sachse, M., Klumperman, J., and Strous, G. (2001) *J. Biol. Chem.* **276,** 3778–3784
28. Lippincott-Schwartz, J., Presley, J., Zaal, K., Hirschberg, K., Miller, C., and Ellenberg, J. (1999) *Methods Cell Biol.* **58,** 261–281
29. Reits, E., and Neefjes, J. (2001) *Nat. Cell Biol.* **3,** 145–147
30. Touret, N., Furuya, W., Forbes, J., Gros, P., and Grinstein, S. (2003) *J. Biol. Chem.* **278,** 25548–25557
31. Su, T., Cariappa, R., and Stanley, K. (1999) *FEBS Lett.* **453,** 391–394
32. Haller, C., Kiessling, F., and Kubler, W. (1997) *Eur. J. Cell Biol.* **75,** 353–361
33. Lidell, M., Johansson, M., and Hansson, G. (2003) *J. Biol. Chem.* **278,** 13944–13951
34. Machen, T., Leigh, M., Taylor, C., Kimura, T., Asano, S., and Moore, H. (2003) *Am. J. Physiol. Cell Physiol.* **285,** 205–214
35. Wu, M., Grabe, M., Adams, S., Tsien, R., Moore, H., and Machen, T. (2001) *J. Biol. Chem.* **276,** 33027–33035
36. Kim, J., Johannes, L., Goud, B., Antony, C., Lingwood, C., Daneman, R., and Grinstein, S. (1998) *Proc. Natl. Acad. Sci. U. S. A.* **95,** 2997–3002
37. Takahashi, K., Sawasaki, Y., Hata, J., Mukai, K., and Goto, T. (1990) *In Vitro Cell. Dev. Biol.* **25,** 265–274
38. Takahashi, K., and Sawasaki, Y. (1992) *In Vitro Cell. Dev. Biol.* **28,** 380–382
39. Hughes, S. (1996) *Exp. Cell Res.* **225,** 171–185
40. Volk, R., Schwartz, J., Li, J., Rosenberg, R., and Simons, M. (1999) *J. Biol. Chem.* **274,** 24417–24424
41. Kishibe, J., Yamada, S., Okada, Y., Sato, J., Ito, A., Miyazaki, K., and Sugahara, K. (2000) *J. Biol. Chem.* **275,** 15321–15329
42. Lucas, A., Chadwick, N., Warren, B., Jewell, D., Gordon, S., Powrie, F., and Greaves, D. (2001) *Am. J. Pathol.* **158,** 855–866
43. Yoshikawa, M., Nakajima, T., Matsumoto, K., Okada, N., Tsukidate, T., Iida, M., Otori, N., Haruna, S., Moriyama, H., Imai, T., and Saito, H. (2004) *FEBS Lett.* **561,** 105–110
44. Umehara, H., Bloom, E., Okazaki, T., Domae, N., and Imai, T. (2001) *Trends Immunol.* **22,** 602–607
45. Garton, K., Gough, P., Blobel, C., Murphy, G., Greaves, D., Dempsey, P., and Raines, E. (2001) *J. Biol. Chem.* **276,** 37993–38001
46. Hundhausen, C., Misztela, D., Berkhout, T., Broadway, N., Saftig, P., Reiss, K., Hartmann, D., Fahrenholz, F., Postina, R., Matthews, V., Kallen, K.-J., Rose-John, S., and Ludwig, A. (2003) *Blood* **102,** 1186–1195
47. Tsou, C.-L., Haskell, C., and Charo, I. (2001) *J. Biol. Chem.* **276,** 44622–44626
48. Sheff, D., Pelletier, L., O'Connell, C., Warren, G., and Mellman, I. (2002) *J. Cell Biol.* **156,** 797–804
49. Daro, E., van der Sluijs, P., Galli, T., and Mellman, I. (1996) *Proc. Natl. Acad. Sci. U. S. A.* **18,** 9559–9564
50. McCaffrey, M., Bielli, A., Cantalupo, G., Mora, S., Roberti, V., Santillo, M., Drummond, F., and Bucci, C. (2001) *FEBS Lett.* **495,** 21–30
51. Ward, E., Martinez, C., Vaccaro, C., Zhou, J., Tang, Q., and Ober, R. (2005) *Mol. Biol. Cell* **16,** 2028–2038
52. Zhang, X., Ellis, S., Sriratana, A., Mitchell, C., and Rowe, T. (2004) *J. Biol. Chem.* **279,** 43027–43034
53. Yao, X., and Forte, J. (2003) *Annu. Rev. Physiol.* **65,** 103–131
54. Pastor-Soler, N., Beaulieu, V., Litvin, T., Da Silva, N., Chen, Y., Brown, D., Buck, J., Levin, L., and Breton, S. (2003) *J. Biol. Chem.* **278,** 49523–49529
55. Rudich, A., and Klip, A. (2003) *Acta Physiol. Scand.* **178,** 297–308
56. Govers, R., Coster, A., and James, D. (2004) *Mol. Cell. Biol.* **14,** 6456–6466
57. Schlondorff, J., Becherer, J., and Blobel, C. (2000) *Biochem. J.* **347,** 131–138
58. Hatsuzawa, K., Nagahama, M., Takahashi, S., Takada, K., Murakami, K., and Nakayama, K. (1992) *J. Biol. Chem.* **267,** 16094–16099
59. Stieneke-Grober, A., Vey, M., Angliker, H., Shaw, E., Thomas, G., Roberts, C., Klenk, H., and Garten, W. (1992) *EMBO J.* **11,** 2407–2414
60. Zhou, Y., and Lindberg, I. (1993) *J. Biol. Chem.* **268,** 5615–5623
61. Sun, T., Van Hoek, A., Huang, Y., Bouley, R., McLaughlin, M., and Brown, D. (2002) *Am. J. Physiol. Renal Physiol.* **282,** 998–1011
62. Katsura, T., Ausiello, D., and Brown, D. (1996) *Am. J. Physiol. Renal Fluid Electrolyte Physiol.* **270,** 548–553
63. Jhun, B., Rampal, A., Liu, H., Lachaal, M., and Jung, C. (1992) *J. Biol. Chem.* **267,** 17710–17715